BOLD-MRI in patients with type 2 diabetes. *Diabetes Res Clin Pract* 2013; 99: 136–144
22. Siddiqi L, Hoogduin H, Visser F *et al.* Inhibition of the renin-angiotensin system affects kidney tissue oxygenation evaluated by magnetic resonance imaging in patients with chronic kidney disease. *J Clin Hypertens* 2014; 16: 214–218
23. Djamali A, Sadowski EA, Muehrer RJ *et al.* BOLD-MRI assessment of intra-renal oxygenation and oxidative stress in patients with chronic kidney allograft dysfunction. *Am J Physiol Renal Physiol* 2007; 292: F513–F522
24. Epstein FH, Prasad P. Effects of furosemide on medullary oxygenation in younger and older subjects. *Kidney Int* 2000; 57: 2080–2083
25. Prasad PV, Epstein FH. Changes in renal medullary pO2 during water diuresis as evaluated by blood oxygenation level-dependent magnetic resonance imaging: effects of aging and cyclooxygenase inhibition. *Kidney Int* 1999; 55: 294–298
26. Tumkur SM, Vu AT, Li LP *et al.* Evaluation of intra-renal oxygenation during water diuresis: a time-resolved study using BOLD MRI. *Kidney Int* 2006; 70: 139–143
27. Milani B, Ansaloni A, Sousa-Guimaraes S *et al.* Reduction of cortical oxygenation in chronic kidney disease: evidence obtained with a new analysis method of blood oxygenation level-dependent magnetic resonance imaging. *Nephrol Dial Transplant* 2016; 32: 2097–2105

Received: 14.4.2018; Editorial decision: 12.9.2018

Nephrol Dial Transplant (2020) 35: 970–978
doi: 10.1093/ndt/gfz066
Advance Access publication 23 April 2019

The utility of magnetic resonance imaging for noninvasive evaluation of diabetic nephropathy

Robert S. Brown[1], Maryellen R. M. Sun[2], Isaac E. Stillman[3], Teresa L. Russell[4], Sylvia E. Rosas[5,6] and Jesse L. Wei[4]

[1]Division of Nephrology, Beth Israel Deaconess Medical Center and Harvard Medical School, Boston, MA, USA, [2]Department of Radiology, Lowell General Hospital, Lowell, MA, USA, [3]Department of Pathology, Beth Israel Deaconess Medical Center and Harvard Medical School, Boston, MA, USA, [4]Department of Radiology, Beth Israel Deaconess Medical Center and Harvard Medical School, Boston, MA, USA and [5]Kidney and Hypertension Unit, Joslin Diabetes Center, Boston, MA, USA and [6]Division of Nephrology, Beth Israel Deaconess Medical Center, Harvard Medical School, Boston, MA, USA

Correspondence and offprint requests to: Robert S. Brown; E-mail: rbrown@bidmc.harvard.edu

ABSTRACT

Background. Noninvasive quantitative measurement of fibrosis in chronic kidney disease (CKD) would be desirable diagnostically and therapeutically but standard radiologic imaging is too variable for clinical usage. By applying a vibratory force, tissue shear wave stiffness can be measured by magnetic resonance elastography (MRE) that may correlate with progression of kidney fibrosis. Since decreased kidney perfusion decreases tissue turgor and stiffness, we combined newly available three-dimensional MRE shear stiffness measurements with MR arterial spin labeling (ASL) kidney blood flow rates to evaluate fibrosis in diabetic nephropathy.

Methods. Thirty individuals with diabetes and Stage 0–5 CKD and 13 control individuals without CKD underwent noncontrast MRE with concurrent ASL blood flow measurements.

Results. MRE cortical shear stiffness at 90 Hz was decreased significantly below controls in all CKD stages of diabetic nephropathy. Likewise, ASL blood flow decreased progressively from 480 ± 136 mL/min/100 g of cortical tissue in controls to 302 ± 95, 229 ± 7 and 152 ± 32 mL/min/100 g in Stages 3, 4 and 5 CKD, respectively. A magnetic resonance imaging (MRI) surrogate for the measured glomerular filtration fraction [surrogate filtration fraction = estimated glomerular filtration rate (eGFR)/ASL] decreased progressively from 0.21 ± 0.07 in controls to 0.16 ± 0.04 in Stage 3 and 0.10 ± 0.02 in Stage 4–5 CKD.

Conclusions. In this pilot study, MRI with ASL blood flow rates can noninvasively measure decreasing kidney cortical tissue perfusion and, with eGFR, a decreasing surrogate filtration fraction in worsening diabetic nephropathy that appears to correlate with increasing fibrosis. Differing from the liver, MRE shear stiffness surprisingly decreases with worsening CKD, likely related to decreased tissue turgor from lower blood flow rates.

Keywords: chronic kidney disease, diabetic nephropathy, kidney fibrosis, kidney perfusion, magnetic resonance elastography

ADDITIONAL CONTENT

An author video to accompany this article is available at: https://academic.oup.com/ndt/pages/author_videos.

INTRODUCTION

Diabetes is the most common etiology of chronic kidney disease (CKD) [1] and kidney fibrosis is a key component of the final common pathway leading to end-stage kidney disease [2, 3]. Current screening markers, such as serum creatinine and cystatin C, provide an estimate of the glomerular filtration rate (GFR) but only a rough approximation of the overall degree of permanent anatomical damage. Because the failing kidney is able to compensate up to a point, there may be significant kidney fibrosis unaccompanied by measurable changes in GFR or there may be decreases in GFR without significant scarring. Knowing the degree of anatomical damage would be useful to assess treatment response in patients with progressive diabetic nephropathy, but serial kidney biopsies are unrealistic.

Previous attempts at noninvasive imaging to measure kidney fibrosis with multiple radiologic techniques have shown varying results [4–13]. Since magnetic resonance elastography (MRE) has shown success in quantitating the increased shear stiffness of liver tissue in the setting of hepatic fibrosis and cirrhosis [14, 15], we decided to apply newly available three-dimensional (3D) MRE in a pilot study to evaluate parenchymal stiffness for evaluation of kidney fibrosis in diabetic nephropathy compared with normal controls. Because parenchymal stiffness is influenced by the degree of tissue perfusion [16] and decreased renal blood flow may mask the presence of fibrosis [17], kidney perfusion was measured using magnetic resonance arterial spin labeling (ASL), an imaging technique to quantitate the perfusion of tissues without the need for intravenous contrast [10, 11, 18–20]. Using ASL, the water component of blood supplying the kidneys is 'labeled' within the suprarenal aorta using a magnetic resonance imaging (MRI) pulse sequence. Imaging of a selected portion of the kidney is performed both without and after the labeling, with the difference in signal between the two acquisitions resulting from the labeling ('perfusion difference'), allowing for automated calculation of quantitative perfusion on a per-voxel basis. As measured by ASL, a recent report [21] has shown a significant decrease in kidney tissue perfusion in Stage 3 CKD due to diabetes. We linked the MRE assessment of stiffness with the ASL measurement of tissue perfusion, resulting in a novel noninvasive evaluation of diabetic nephropathy.

MATERIALS AND METHODS

Study participants

We recruited 30 patients with diabetes not on dialysis, of whom 5 patients were recruited after a clinically indicated kidney biopsy had shown diabetic nephropathy. Twenty-eight of the 30 patients had Stage 1–5 CKD clinically attributed to diabetic nephropathy (seven with type 1 diabetes). Thirteen normal volunteers with urinary albumin:creatinine levels of <25 mg/g, normal serum creatinine levels and normal eGFRs for age (calculated by the Chronic Kidney Disease Epidemiology Collaboration formula [22, 23]) were recruited as control participants. Study subject inclusion criteria were stable adult outpatients with diabetes without acute kidney injury. Exclusions were relative contraindications to MRI, including claustrophobia, pregnancy or unsuitability for informed consent. No intravenous contrast agent or other medications were given with the MRI. The study was approved by the Committee on Clinical Investigations of the Beth Israel Deaconess Medical Center, was Health Insurance Portability and Accountability Act compliant with informed consent by every participant and had no related adverse events.

MRI of kidney shear stiffness and blood flow

MRE examinations were performed on a 1.5 T MRI magnet (Signa HDxt, GE, Waukesha, WI, USA) with a mechanical MRE apparatus and a software package that was provided for pulse sequence, imaging reconstruction and image inversion for elastography calculation (available via Research Agreement, Mayo Clinic, Rochester, MN, USA). An external 12-channel phased-array torso coil was used for signal reception. Patients were positioned supine and two identical passive acoustic drivers were placed posteriorly corresponding to the locations of the right and left kidneys and held in position against the skin with foam padding and an elastic fixation belt.

After conventional anatomic localizer sequences were performed, multiparametric noncontrast imaging was performed through each kidney. MRE was performed with acoustic energy transmitted from an active elastography driver located outside of the scan room, with polyvinylchloride tubing serving as a waveguide and connected to each passive driver using a Y-fitting. The passive drivers, tightly strapped to the patient, allowed coupling of mechanical wave propagation through the body, which was detected by the MRE pulse sequences and post-processing software. Mechanical vibration frequencies of 60 and 90 Hz were applied in synchrony with the MRE pulse sequence: a multislice, flow-compensated, two-dimensional spin-echo planar imaging (EPI) sequence with motion-encoding gradients in the three orthogonal cardinal directions [repetition time (TR)/echo time (TE) 1000/54 ms, matrix 96×96, field of view (FOV) 40 cm, slice thickness 3mm) [24].

Shear stiffness measurements were performed with the OsiriX DICOM image viewer program [25] via placement of a freeform Bezier polygonal region of interest, to include at least 50% of the representative renal cortex of each kidney as visualized on a single coronal image slice, while attempting to exclude the renal medulla, renal sinus, extrarenal fat and regions of imaging artifact. The boundaries of the renal cortex were identified and drawn on the anatomic 'magnitude images'; these regions of interest were then digitally propagated onto corresponding stiffness maps created by the elastography postprocessing pipeline (Supplementary data, Figure S1). Mean shear stiffness values within the cortical region of interest were measured in Pascals (Pa) as separate analyses for each kidney in each study subject.

ASL was performed in the axial plane through the center of each kidney using single-shot fast spin-echo with pseudocontinuous labeling as previously reported [19]. Single-shot fast spin-echo images were obtained for control images and labeling was performed in an axial plane 8–10 cm upstream from the level of the renal arteries in the upper abdominal aorta for 1500 ms followed by a 1500-ms postlabeling delay (TR/TE 6000/50 ms, matrix 128×128, FOV 40 cm, slice thickness 10 mm, receiver bandwidth ±19.23 kHz). A repetition time of

6 seconds was used to allow for recovery of blood signal. Patients were instructed to breathe in synchrony between the 6-s acquisitions and imaging was acquired over ∼2 min of coached respiration. The software postprocessing pipeline resulted in output images including proton density anatomic images as well as quantitative perfusion maps (calculated based on calculated tissue T1 characteristics) with voxel intensity representing perfusion per unit volume (mL/min/100 g tissue).

Similar to the MRE stiffness measurements, renal perfusion analysis was performed using OsiriX software, with the cortical volume for perfusion analysis determined by drawing regions of interest around each cortex on proton density-weighted reference images and digitally propagated to the accompanying quantitative perfusion images. In cases where there was misregistration between the proton density-weighted reference images and the perfusion images, the cortex was adjusted to correspond to the visual cortical morphology on the perfusion difference and quantitative perfusion images (Supplementary data, Figure S2).

Kidney biopsy analysis

The five kidney biopsies with diabetic nephropathy were evaluated for interstitial fibrosis by a renal pathologist who was blinded to the clinical and MRE data. Five slides, cut at various levels through the fixed block of kidney tissue, were stained with Masson's trichrome and overall cortical fibrosis of those slides was graded as follows:

Grade 0: no interstitial fibrosis or tubular atrophy (<5% of cortical area)
Grade I: mild interstitial fibrosis and tubular atrophy (6–25% of cortical area)
Grade II: moderate interstitial fibrosis and tubular atrophy (26–50% of cortical area)
Grade III: severe interstitial fibrosis and tubular atrophy/loss (51–90% of cortical area)
Grade IV: advanced interstitial fibrosis and tubular atrophy/loss (>90% of cortical area)

Surrogate filtration fraction

We calculated an imaging-based surrogate for the glomerular filtration fraction, defined as the ratio of the GFR to the renal plasma flow, by utilizing the creatinine-based calculated eGFR divided by the measured ASL renal blood flow rate, creating a surrogate filtration fraction (sFF; sFF = eGFR/ASL). Three main systematic differences distinguish the sFF from an actual filtration fraction: (i) ASL flow rate measures whole blood rather than renal plasma flow, thereby an increased flow rate will reduce the sFF; (ii) ASL blood flow measurement was of the renal cortex with its greater flow rate than the medulla, thereby an increased flow rate will also reduce the sFF and (iii) ASL blood flow measurement, normalized to 100 g of kidney cortex rather than ∼200 g of weight for each kidney (average of 170–227 g in different populations [26–28]) will yield a lower flow rate that will increase the sFF. These differences tend to cancel out each other, resulting in sFFs in the controls that were close to actual normal filtration fraction values. Of course, the differences between the sFF and a filtration fraction based on measured GFR and renal plasma flow will depend upon the above variable factors, but in any event, the sFF would be expected to be reasonably proportional to the actual measured glomerular filtration fraction (as described in Supplementary data, Figure S3).

Statistical analyses

We calculated Spearman rank correlations using the raw data to examine the association between MR shear stiffness and ASL perfusion measurements, right and left kidneys and of shear stiffness and ASL blood flow rates with eGFR. The mean and standard deviation of imaging acquisitions and sFF data were calculated for the normal controls and patients with diabetic nephropathy separated into groups based on the stage of CKD. Comparisons of these groups with the normal controls were made with Student's *t*-test with two-sided P-values.

RESULTS

MRE findings

3D MRE cortical shear stiffness measurements obtained at an applied tissue vibration frequency of either 60 or 90 Hz showed that the left kidney correlated closely with the right kidney of each control and diabetic study participant (Supplementary data, Figure S4). Although shear stiffness of kidneys at 60 Hz decreased somewhat with worsening diabetic nephropathy, measurement at this vibration frequency failed to distinguish Stage 3, 4 or 5 CKD from normal controls (Figure 1A). However, at 90 Hz, MRE showed a progressive decrease of stiffness with worsening diabetic nephropathy, with Stage 3, 4 and 5 CKD patients having significantly lower measurements than the normal controls (Tables 1 and 2, Figure 1B). MRE shear stiffness was weakly positively correlated with eGFR levels at 60 Hz ($r = 0.25$, $P = 0.025$) and more strongly at 90 Hz ($r = 0.41$, $P \leq 0.001$).

ASL renal blood flow findings

ASL-measured renal blood flow per 100 g of cortical tissue to the left kidney correlated very closely with the right kidney of each study participant (Supplementary data, Figure S5). ASL blood flow rates decreased significantly with worsening diabetic nephropathy, from 480 ± 136 mL/min/100 g in normal controls to 302 ± 95, 229 ± 7, and 152 ± 32 mL/min/100 g in Stage 3, 4 and 5 CKD, respectively (Tables 1 and 2). ASL blood flow rates were strongly positively correlated with eGFR levels ($r = 0.70$, $P \leq 0.001$; Figure 2A), as well as with MRE shear stiffness at 90 Hz ($r = 0.52$, $P \leq 0.001$; Figure 2B). A comparison of MRE shear stiffness with ASL blood flow rates by CKD stages of diabetic nephropathy is shown in Figure 3.

sFF

The surrogate for the glomerular filtration fraction, sFF = eGFR/ASL blood flow rate, was found to be an average of 0.21 ± 0.07 in the normal controls (Table 2). The sFF was progressively lower with decreasing eGFR in both the normal controls and the patients with worsening diabetic nephropathy, decreasing significantly to 0.16 ± 0.04 in Stage 3 and 0.10 ± 0.02 in Stages 4 and 5 CKD (Table 2 and Figure 4). Although not prospectively controlled for in this pilot study, the sFF did not appear to be largely affected by renin–

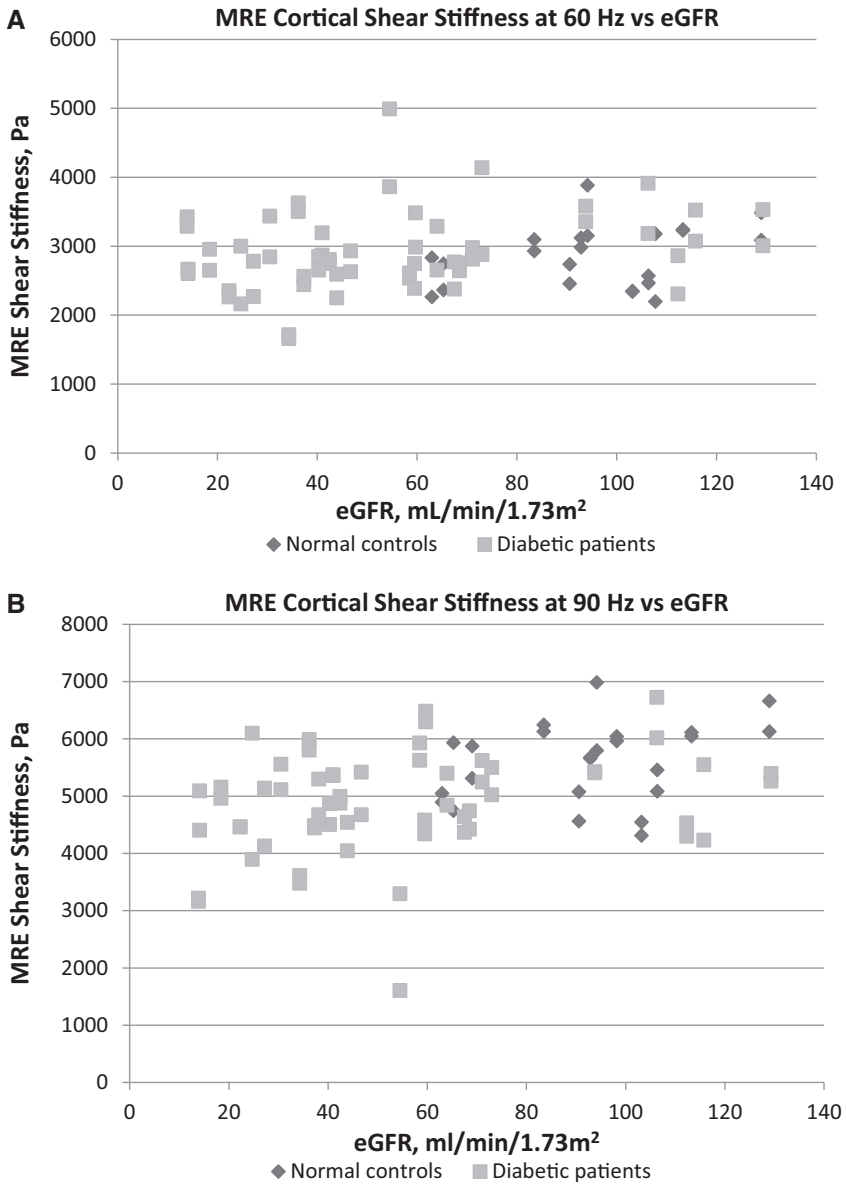

FIGURE 1: 3D MRE cortical shear stiffness plotted by eGFR levels: (**A**) in 11 normal controls and 29 diabetic patients (80 total kidneys) at 60 Hz and (**B**) in 12 normal controls and 30 diabetic patients (84 total kidneys) at 90 Hz.

Table 1. Results of MRE shear stiffness (3D at 90 Hz) and renal blood flow by ASL in normal controls and patients with diabetes grouped by CKD stage based on eGFR

Participant group ($N = 43$)	Age, mean ± SD	Sex (M/F), n/n	Race (AA/non-AA), n/n	eGFR (mL/min/1.73 m^2), mean ± SD	Shear stiffness (Pa; 3D, 90 Hz), mean ±SD		ASL perfusion (mL/min/100 g tissue), mean ± SD	
					Right kidney	Left kidney	Right kidney	Left kidney
Normal controls ($n = 13$	50 ± 17	7/6	1/12	94 ± 20	5784 ± 687 ($n = 12$)	5401 ± 673 ($n = 12$)	491 ± 158 ($n = 12$)	468 ± 117 ($n = 12$)
Diabetes, no nephropathy ($n = 2$)	61 ± 4	2/0	0/2	100 ± 9	6076 ± 919	5709 ± 432	584 ($n = 1$)	601 ($n = 1$)
CKD Stage 1 ($n = 3$)	44 ± 15	2/1	2/1	119 ± 9*	4674 ± 530*	5078 ± 680	446 ± 180	399 ± 130
CKD Stage 2 ($n = 5$)	64 ± 9	1/4	2/3	69 ± 4*	5179 ± 453	4778 ± 380	405 ± 136	379 ± 123
CKD Stage 3 ($n = 14$)	65 ± 8	10/4	2/12	45 ± 10***	4878 ± 1184*	4780 ± 877	310 ± 110**	294 ± 80***
CKD Stage 4 ($n = 4$)	68 ± 10	2/2	0/4	23 ± 4***	5163 ± 686	4409 ± 550*	228 ± 10* ($n = 3$)	231 ± 3* ($n = 2$)
CKD Stage 5 ($n = 2$)	60 ± 29	1/1	1/1	14 ± 0.1***	4126 ± 1365*	3809 ± 837*	161 ± 14*	143 ± 51**

Significance in comparisons of means with the normal controls: *P ≤ 0.05, **P ≤ 0.01, ***P ≤ 0.001.
AA, African American.

Table 2. Results of MR ASL renal blood flow, sFF = eGFR/ASL and 3D MRE shear stiffness in kidneys of normal controls and patients with diabetes grouped by CKD stage

Participant group	ASL (mL/min/100 g), mean ± SD, n = Number of kidneys	Surrogate filtration fraction mean ± SD, n = number of subjects	Shear stiffness (Pa, 3D, 90 Hz), mean ± SD, n = number of kidneys
Normal controls	480 ± 136, $n = 24$	0.21 ± 0.07, $n = 12$	5592 ± 693, $n = 24$
Diabetes, no nephropathy	593 ± 12, $n = 2$	0.18, $n = 1$	5892 ± 623, $n = 4$
CKD Stage 1	446 ± 161, $n = 6$	0.31 ± 0.10*, $n = 3$	4876 ± 589*, $n = 6$
CKD Stage 2	392 ± 123, $n = 10$	0.19 ± 0.07, $n = 5$	4978 ± 447*, $n = 10$
CKD Stage 3	302 ± 95***, $n = 28$	0.16 ± 0.04*, $n = 14$	4829 ± 1023**, $n = 28$
CKD Stage 4	229 ± 7**, $n = 5$	0.10 ± 0.02*, $n = 3$	4786 ± 703**, $n = 8$
CKD Stage 5	152 ± 32***, $n = 4$	0.10 ± 0.02*, $n = 2$	3968 ± 942**, $n = 4$

Significance in comparisons of means with normal controls: *P ≤ 0.05, **P ≤ 0.01, ***P ≤ 0.001.

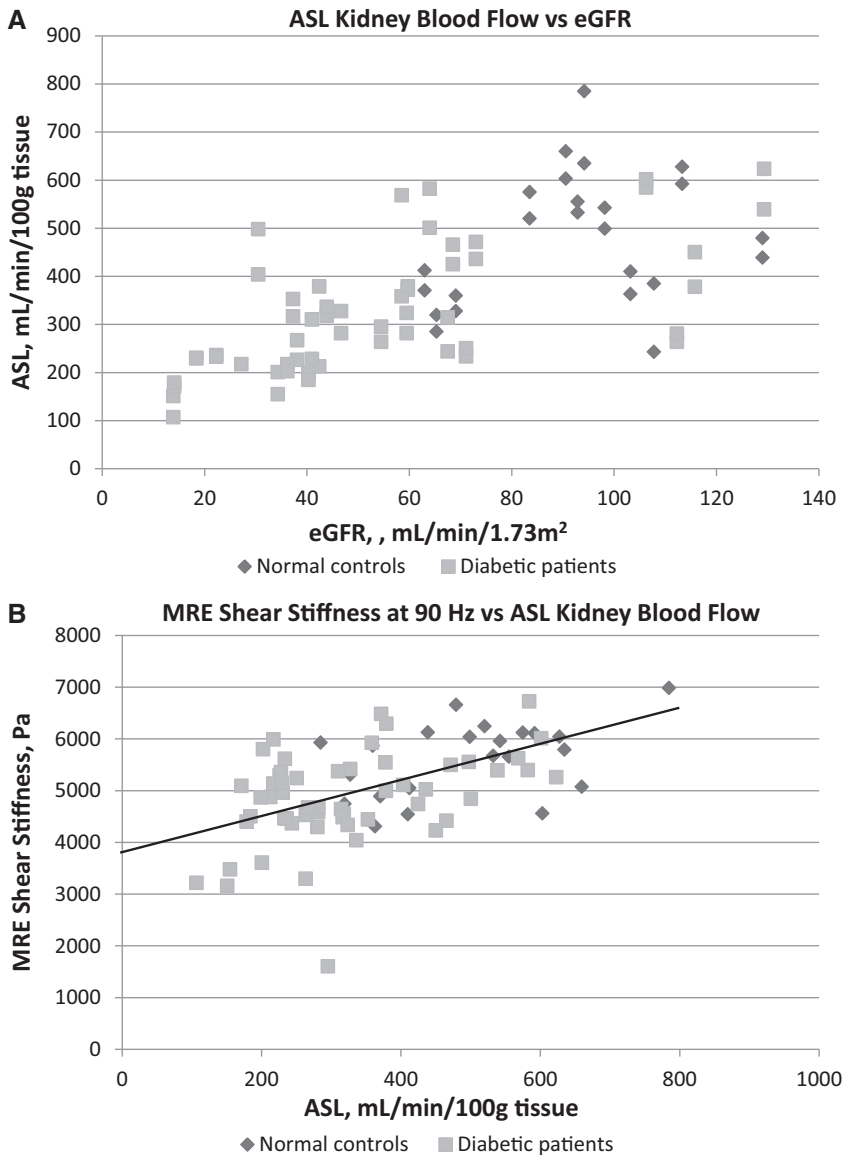

FIGURE 2: MR ASL renal blood flow (**A**) compared with eGFR levels in 12 normal controls and 28 diabetic patients (79 total kidneys) and (**B**) compared with 3D MRE cortical shear stiffness at 90 Hz in 11 normal controls and 28 diabetic patients (77 total kidneys). The solid line depicts the linear regression with an *x*-axis intercept of 3861 Pa, which may represent the residual shear stiffness of the average kidney at zero ASL blood flow rate.

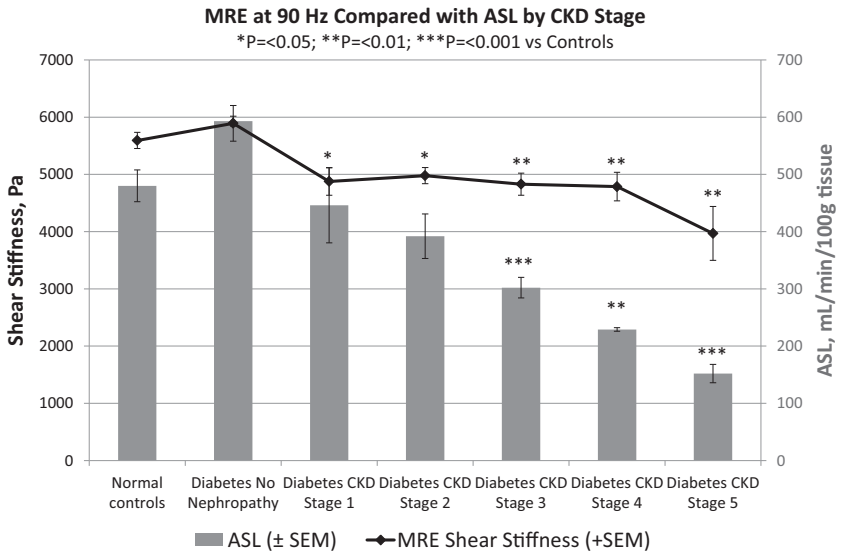

FIGURE 3: 3D MRE cortical shear stiffness at 90 Hz compared with ASL cortical blood flow in kidneys of normal controls and patients with diabetes grouped by CKD stage. Both MRE shear stiffness and ASL blood flow decrease significantly with worsening diabetic nephropathy, but separation of CKD stages is more clearly shown by ASL blood flow.

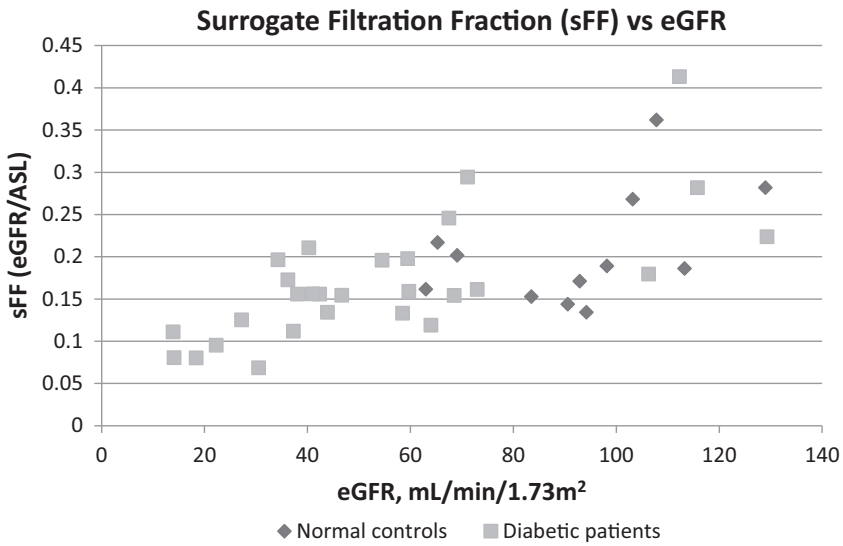

FIGURE 4: sFF = eGFR/ASL renal blood flow plotted against eGFR in 12 normal controls and 28 diabetic patients. The sFF decreases with decreasing GFR in the normal controls and diabetic patients.

angiotensin system blockers (Supplementary data, Figure S6). The sFF was noted to be significantly higher in the diabetic patients with Stage 1 CKD (Table 2).

Association of kidney biopsy fibrosis with MRE shear stiffness and ASL renal blood flow

Pathology results from a renal biopsy were available for five patients in the diabetic nephropathy group (Table 3). There was little difference in MRE shear stiffness between Grade II and III interstitial fibrosis, although the measured shear stiffness was noted to be lower in the one patient's kidney with Grade IV interstitial fibrosis. There was a more clear decrease in ASL tissue perfusion with increasing grades of interstitial fibrosis, from an average of 352 mL/min/100 g in Grade II to 201 mL/min/100 g in Grade III and 107 mL/min/100 g in Grade IV interstitial fibrosis.

DISCUSSION

With diabetes as the most common cause of the increasing prevalence of CKD [1], the noninvasive detection of kidney fibrosis [2, 3] using MRI might have an impact on the evaluation of therapies to prevent progression of CKD and fibrosis [2, 29–31]. This is timely as a potential means to evaluate the efficacy of antifibrotic agents in development, particularly if they decrease eGFR without affecting anatomical fibrosis. Unfortunately, conventional radiologic imaging with ultrasound, CT or MRI has had variable results in assessing fibrosis to date [4–13].

Table 3. Results of interstitial fibrosis grade by kidney biopsy compared with eGFR, MRE shear stiffness and ASL renal blood flow in five diabetic patients with Stage 2–5 CKD due to diabetic nephropathy

Kidney fibrosis grade by biopsy	Time from biopsy date to MRE study (right or left kidney)	eGFR (mL/min/ 1.73 m^2)	Shear stiffness right kidney (Pa at 90 Hz)	Shear stiffness left kidney (Pa at 90 Hz)	ASL perfusion right kidney (mL/min/ 100 g)	ASL perfusion left kidney (mL/min/ 100 g)
II	41 days (left)	73	5496	**5021**	472	**436**
II	47 days (left)	38	5297	**4673**	226	**267**
III	86 days (left)	36	5988	**5800**	217	**202**
III	44 days (right)	40	**4866**	4502	**199**	184
IV	42 days (left)	14	3161	**3217**	151	**107**

Tissue perfusion by measured ASL blood flow decreases more clearly than MR shear stiffness with increasing fibrosis by biopsy in this small sample. The bold figures demarcate results for biopsied kidney.

We explored noninvasive imaging of diabetic nephropathy with a combination of kidney stiffness measurements using MRE and blood flow measurements using MR ASL. Due to the unpredictable direction of shear wave propagation when performing MRE, we used a 3D MRE technique to minimize quantitative artifacts related to varying directionality of wave propagation. We found that the reliability of MRE for native kidneys [32] was improved at a mechanical excitation frequency of 90 Hz rather than 60 Hz, likely related to improved quantification of the thin renal cortex related to the shorter wavelength of 90 Hz excitation compared with 60 Hz.

Somewhat unexpectedly, we found that MR shear stiffness in diabetic nephropathy decreases significantly with decreased kidney function, distinguishing Stage 3–5 CKD from normal controls. Differing from our findings, MRE of renal allografts was reported to have higher shear stiffness with increased fibrosis by biopsy [7, 9]. However, similar to our data, MRE shear stiffness correlated positively with eGFR and functioning allografts had higher shear stiffness than both dysfunctional allografts and native kidneys [8, 13]. Since experimental models in pigs have shown that acutely decreasing renal blood flow to produce renal ischemia causes a decrease in MRE shear stiffness [17], we suspected that the decreased blood flow reported previously in CKD Stage 3 diabetic nephropathy [21] had the same effect upon MR shear stiffness in our study. This blood flow effect on kidney turgor would also serve to explain the decrease in MR shear stiffness reported for nonfunctioning renal allografts [8]. So it was not surprising that our simultaneous ASL cortical blood flow measurements showed markedly decreasing kidney perfusion with worsening diabetic nephropathy. It is likely that the decreased ASL blood flow per 100 g of cortical tissue rather than total kidney blood flow represents areas of nonfunctioning nephrons and may well correlate with interstitial fibrosis. This decrease in perfusion might contribute to progressive CKD by causing renal hypoxia, as low cortical oxygenation shown by blood oxygenation level–dependent (BOLD) MRI in CKD patients was reported to correlate with greater decreases in eGFR over time [33]. Since nonlinear progression of CKD is relatively common in diabetic nephropathy [34], it remains to be seen in larger longitudinal studies whether noninvasive ASL renal blood flow alone or with additional tissue characterization added by MRE shear stiffness measurements is a useful marker to detect patients with different rates of progressive kidney disease despite similar eGFRs.

Our pilot study utilized noninvasive MR measurement of kidney blood flow rates to calculate a surrogate for the glomerular filtration fraction, the sFF. The significantly higher sFF noted in the diabetic patients with Stage 1 CKD likely indicates hyperfiltering glomeruli seen in early diabetic kidneys [35], whereas the sFF decreased markedly with decreasing eGFR in worsening diabetic nephropathy. A decrease in filtration fraction is counter to the response of a normal kidney in which a decreased renal blood flow rate from hypotension [36] or hypovolemia [37] will result in an increased glomerular filtration fraction. However, our results showing a decrease in sFF are quite similar to a study of 62 CKD patients (average eGFR 36 ± 23 mL/min/1.73 m^2, 14 with diabetic nephropathy) using phase contrast MRI and chromium-51-labeled ethylenediaminetetraacetic acid plasma clearance in which filtration fraction decreased from 0.18 in controls to 0.09 in patients [38]. Those authors postulated that their finding of a decrease in glomerular filtration fraction in CKD patients, and thereby a decrease in tubular sodium reabsorptive energy requirements, may serve to prevent renal hypoxia in CKD in the setting of lower tissue oxygenation [38]. A recent report [39] using BOLD MRI noted a surprising increase in oxygenation in the renal medulla (where oxygenation is lowest) when renal blood flow was reduced by handgrip exercise. Thus the decrease of sFF and its relation to the decrease in ASL perfusion may serve an important protective function in the progression of diabetic nephropathy.

While our study has many strengths, including state-of-the-art MRE/ASL as well as histological validation, we acknowledge several limitations. The pilot study is relatively small, with only 30 patients with diabetes and five kidney biopsies, but our results appear to be significant and convincing. Also, the reproducibility of ASL blood flow rates has been reported previously [40] and is consistent with our strong correlation between left and right kidney flow rates. However, ASL blood flow rates expressed per 100 g of cortical tissue cannot necessarily be extrapolated to overall renal blood flow rates without accounting for differences in kidney sizes and overall cortical volume among individuals of different size and sex [41]. A similar limitation might affect the sFF in addition to the well-described relative variation of eGFR determinations compared with measured GFRs [42]. This is particularly true for eGFRs >90 mL/min/1.73 m^2, where eGFR tends to underestimate the GFR so that the sFF, and thereby hyperfiltration, may be

underestimated [42]. The patients with diabetes and no nephropathy based on normal kidney function and no albuminuria may have undiscovered diabetic nephropathy, as has been described at autopsy [43]. The conflicting differences of MRE shear stiffness results in failing kidney allografts may depend upon technique or a greater degree of fibrosis in allografts. Also, we cannot assume that these results will be similar for other etiologies of CKD, those in whom renal mass weight is less than in patients with diabetic nephropathy [41].

In summary, we propose that noninvasive MRI with ASL renal blood flow rates may provide a useful tool to characterize patients with worsening diabetic nephropathy. The measurement of decreasing tissue perfusion and decreasing surrogate glomerular filtration fraction rates appear likely to be associated with increasing interstitial kidney fibrosis. Unlike the findings reported for the liver and some transplant kidney studies, MRE shear stiffness surprisingly decreases with worsening CKD in diabetic nephropathy, likely related to the partial dependence of kidney stiffness upon perfusional turgor linked to the decreasing ASL blood flow rates. Larger longitudinal studies will be needed to elucidate how these data will add to estimated GFRs to be of clinical value in assessing prognosis and therapeutic interventions.

SUPPLEMENTARY DATA

Supplementary data are available at ndt online.

ACKNOWLEDGEMENTS

The authors acknowledge the expertise of Richard L. Ehman, MD, PhD, and Kevin J. Glaser, PhD (Mayo Clinic) in planning the kidney MRE, the assistance of David C. Alsop, PhD and Manuel Taso, PhD in planning and processing the ASL imaging, the research assistance of Bridget Giarusso and Meaghan Fox in study subject scheduling, MR safety and accrual and organization of data.

FUNDING

The study was funded by Harvard Catalyst (Subaward 027242.386541.0501) and by a DiaComp Pilot and Feasibility Study, National Institute of Diabetes and Digestive and Kidney Diseases, 'MR Elastography for Noninvasive Assessment of Fibrosis in Diabetic Kidney Disease' (Prime Award 3 U24 DK076169-09; Subaward 25732-65), both of which have been completed.

AUTHORS' CONTRIBUTIONS

R.B., J.W. and M.S. designed the study. T.R. and S.R. managed subject accrual and clinical information. J.W. supervised imaging procedures. J.W. and M.S. performed imaging interpretation and measurements. I.S. performed pathology review. R.B. developed the sFF concept, performed statistical analyses and drafted the paper and figures. All authors contributed to edits and revisions of the manuscript and approved the final version of the manuscript.

CONFLICT OF INTEREST STATEMENT

All authors report that they have no relevant conflicts or financial interests. The results presented in this article have not been published previously in whole or in part, except in abstract format.

(See related article by Simms and Sourbron. Recent findings on the clinical utility of renal magnetic resonance imaging biomarkers. *Nephrol Dial Transplant* 2020; 35: 915–919)

REFERENCES

1. Tuttle KR, Bakris GL, Bilous RW *et al.* Diabetic kidney disease: a report from an ADA Consensus Conference. *Diabetes Care* 2014; 37: 2864–2883
2. Boor P, Ostendorf T, Floege J. Renal fibrosis: novel insights into mechanisms and therapeutic targets. *Nat Rev Nephrol* 2010; 6: 643–656
3. Rockey DC, Bell PD, Hill JA. Fibrosis—a common pathway to organ injury and failure. *N Engl J Med* 2015; 372: 1138–1149
4. Inoue T, Kozawa E, Okada H *et al.* Noninvasive evaluation of kidney hypoxia and fibrosis using magnetic resonance imaging. *J Am Soc Nephrol* 2011; 22: 1429–1434
5. Arndt R, Schmidt S, Loddenkemper C *et al.* Noninvasive evaluation of renal allograft fibrosis by transient elastography – a pilot study. *Transpl Int* 2010; 23: 871–877
6. Samir AE, Allegretti AS, Zhu Q *et al.* Shear wave elastography in chronic kidney disease: a pilot experience in native kidneys. *BMC Nephrol* 2015; 16: 119
7. Lee CU, Glockner JF, Glaser KJ *et al.* MR elastography in renal transplant patients and correlation with renal allograft biopsy a feasibility study. *Acad Radiol* 2012; 19: 834–841
8. Garcia SRM, Fischer T, Dürr M *et al.* Multifrequency magnetic resonance elastography for the assessment of renal allograft function. *Invest Radiol* 2016; 51: 591–595
9. Kirpalani A, Hashim E, Leung G *et al.* Magnetic resonance elastography to assess fibrosis in kidney allografts. *Clin J Am Soc Nephrol* 2017; 12: 1671–1679
10. Morrell GR, Zhang JL, Lee VS. Magnetic resonance imaging of the fibrotic kidney. *J Am Soc Nephrol* 2017; 28: 2564–2570
11. Leung G, Kirpalani A, Szeto SG *et al.* Could MRI be used to image kidney fibrosis? a review of recent advances and remaining barriers. *Clin J Am Soc Nephrol* 2017; 12: 1019–1028
12. Li J, An C, Kang L *et al.* Recent advances in magnetic resonance imaging assessment of renal fibrosis. *Adv Chronic Kidney Dis* 2017; 24: 150–153
13. Marticorena Garcia SR, Guo J, Dürr M *et al.* Comparison of ultrasound shear wave elastography with magnetic resonance elastography and renal microvascular flow in the assessment of chronic renal allograft dysfunction. *Acta Radiol* 2018; 59: 1139–1145
14. Toguchi M, Tsurusaki M, Yada N *et al.* Magnetic resonance elastography in the assessment of hepatic fibrosis: a study comparing transient elastography and histological data in the same patients. *Abdom Radiol* 2017; 42: 1659–1666
15. Yin M, Talwalkar JA, Glaser KJ *et al.* Assessment of hepatic fibrosis with magnetic resonance elastography. *Clin Gastroenterol Hepatol* 2007; 5: 1207–1213.e2
16. Yin M, Glaser KJ, Kolipaka A *et al.* Influence of perfusion on tissue stiffness assessed with MR elastography. *Proc Intl Soc Mag Reson Med* 2010; 18: 256
17. Warner L, Yin M, Glaser KJ *et al.* Noninvasive in vivo assessment of renal tissue elasticity during graded renal ischemia using MR elastography. *Invest Radiol* 2011; 46: 509–514
18. Ferré J-C, Bannier E, Raoult H *et al.* Arterial spin labeling (ASL) perfusion: techniques and clinical use. *Diagn Interv Imaging* 2013; 94: 1211–1223
19. Robson PM, Madhuranthakam AJ, Dai W *et al.* Strategies for reducing respiratory motion artifacts in renal perfusion imaging with arterial spin labeling. *Magn Reson Med* 2009; 61: 1374–1387
20. Artz NS, Sadowski EA, Wentland AL *et al.* Arterial spin labeling MRI for assessment of perfusion in native and transplanted kidneys. *Magn Reson Imaging* 2011; 29: 74–82

21. Li L-P, Tan H, Thacker JM *et al.* Evaluation of renal blood flow in chronic kidney disease using arterial spin labeling perfusion magnetic resonance imaging. *Kidney Int Rep* 2017; 2: 36–43
22. Levey AS, Stevens LA, Schmid CH *et al.* A new equation to estimate glomerular filtration rate. *Ann Intern Med* 2009; 150: 604–612
23. Levey AS, Inker LA, Coresh J. GFR estimation: from physiology to public health. *Am J Kidney Dis* 2014; 63: 820–834
24. Murphy MC, Huston J, Jack CR *et al.* Decreased brain stiffness in Alzheimer's disease determined by magnetic resonance elastography. *J Magn Reson Imaging* 2011; 34: 494–498
25. OsiriX DICOM Viewer: the world famous medical imaging viewer. https://www.osirix-viewer.com/ (26 March, 2019, date last accessed)
26. Vasconcelos VD, Katayama RC, Ribeiro MDL *et al.* Kidney weight and volume among living donors in Brazil. *Sao Paulo Med J* 2007; 125: 223–225
27. Cheong B, Muthupillai R, Rubin MF *et al.* Normal values for renal length and volume as measured by magnetic resonance imaging. *Clin J Am Soc Nephrol* 2006; 2: 38–45
28. Codas R, Danjou F, Dagot C *et al.* Influence of allograft weight to recipient bodyweight ratio on outcome of cadaveric renal transplantation. *Nephrology (Carlton)* 2014; 19: 420–425
29. Karihaloo A. Anti-fibrosis therapy and diabetic nephropathy. *Curr Diab Rep* 2012; 12: 414–422
30. Fernandez-Fernandez B, Ortiz A, Gomez-Guerrero C *et al.* Therapeutic approaches to diabetic nephropathy—beyond the RAS. *Nat Rev Nephrol* 2014; 10: 325–346
31. Liu R, Das B, Xiao W *et al.* A novel inhibitor of homeodomain interacting protein kinase 2 mitigates kidney fibrosis through inhibition of the TGF-β1/Smad3 pathway. *J Am Soc Nephrol* 2017; 28: 2133–2143
32. Low G, Owen NE, Joubert I *et al.* Reliability of magnetic resonance elastography using multislice two-dimensional spin-echo echo-planar imaging (SE-EPI) and three-dimensional inversion reconstruction for assessing renal stiffness. *J Magn Reson Imaging* 2015; 42: 844–850
33. Pruijm M, Milani B, Pivin E *et al.* Reduced cortical oxygenation predicts a progressive decline of renal function in patients with chronic kidney disease. *Kidney Int* 2018; 93: 932–940
34. Weldegiorgis M, de Zeeuw D, Li L *et al.* Longitudinal estimated GFR trajectories in patients with and without type 2 diabetes and nephropathy. *Am J Kidney Dis* 2018; 71: 91–101
35. Palatini P. Glomerular hyperfiltration: a marker of early renal damage in pre-diabetes and pre-hypertension. *Nephrol Dial Transplant* 2012; 27: 1708–1714
36. Berdeaux A, Duranteau J, Pussard E *et al.* Baroreflex control of regional vascular resistances during simulated orthostatism. *Kidney Int Suppl* 1992; 37: S29–S33
37. Edouard AR, Degrémont AC, Duranteau J *et al.* Heterogeneous regional vascular responses to simulated transient hypovolemia in man. *Intensive Care Med* 1994; 20: 414–420
38. Khatir DS, Pedersen M, Jespersen B *et al.* Evaluation of renal blood flow and oxygenation in CKD using magnetic resonance imaging. *Am J Kidney Dis* 2015; 661: 402–411
39. Haddock BT, Francis ST, Larsson HBW *et al.* Assessment of perfusion and oxygenation of the human renal cortex and medulla by quantitative MRI during handgrip exercise. *J Am Soc Nephrol* 2018; 29: 2510–2517
40. Artz NS, Sadowski EA, Wentland AL *et al.* Reproducibility of renal perfusion MR imaging in native and transplanted kidneys using non-contrast arterial spin labeling. *J Magn Reson Imaging* 2011; 33: 1414–1421
41. Yang C-C, Chen T-C, Wu C-S *et al.* Sex differences in kidney size and clinical features of patients with uremia. *Gend Med* 2010; 7: 451–457
42. Porrini E, Ruggenenti P, Luis-Lima S *et al.* Estimated GFR: time for a critical appraisal. *Nat Rev Nephrol* 2019; 15: 177–190
43. Klessens CQF, Woutman TD, Veraar KAM *et al.* An autopsy study suggests that diabetic nephropathy is underdiagnosed. *Kidney Int* 2016; 90: 149–156

Received: 23.1.2019; Editorial decision: 13.3.2019